JACS
JOURNAL OF THE AMERICAN CHEMICAL SOCIETY

Article

pubs.acs.org/JACS

Light and Temperature Control of the Spin State of Bis(*p*-methoxyphenyl)carbene: A Magnetically Bistable Carbene

Paolo Costa,[†] Thomas Lohmiller,[†,§] Iris Trosien,[†] Anton Savitsky,[*,§] Wolfgang Lubitz,[§] Miguel Fernandez-Oliva,[‡] Elsa Sanchez-Garcia,[*,‡] and Wolfram Sander[*,†]

[†]Lehrstuhl für Organische Chemie II, Ruhr-Universität Bochum, 44780 Bochum, Germany

[§]Max-Planck-Institut für Chemische Energiekonversion, 45470 Mülheim an der Ruhr, Germany

[‡]Max-Planck-Institut für Kohlenforschung, 45470 Mülheim an der Ruhr, Germany

Supporting Information

ABSTRACT: Bis(*p*-methoxyphenyl)carbene is the first carbene that at cryogenic temperatures can be isolated in both its lowest energy singlet and triplet states. At 3 K, both states coexist indefinitely under these conditions. The carbene is investigated in argon matrices by IR, UV−vis, and X-band EPR spectroscopy and in MTHF glasses by W-band EPR and Q-band ENDOR spectroscopy. UV (365 nm) irradiation of the system results in formation of predominantly the triplet carbene, whereas visible (450 nm) light shifts the photostationary equilibrium toward the singlet state. Upon annealing at higher temperatures (>10 K), the triplet is converted to the singlet; however, cooling back to 3 K does not restore the triplet. Therefore, depending on matrix temperature and irradiation conditions, matrices containing predominantly the triplet or singlet carbene can be generated. Controlling the magnetic and chemical properties of carbenes by using light of different wavelengths might be of general interest for applications such as information storage and radical-initiated polymerization processes.

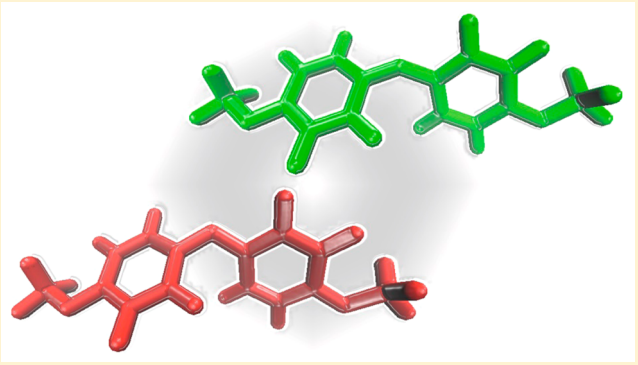

INTRODUCTION

Carbenes are molecules bearing divalent carbon atoms, and the reactivity of these species is highly variable, ranging from the open-shell (triplet or singlet) reactivity expected for a 1,1-diradical to the extreme philicities of closed-shell (singlet) carbenes that resemble 1,1-zwitterions. The stability of carbenes varies from fleeting intermediates with lifetimes in the range of picoseconds to entirely stable compounds that can be isolated at room temperature. The spin-dependent reactivity of carbenes has been subject to intense research for several decades.[1−3]

Very simplified, the electronic structure of a carbene can be described in a two-orbital two-electron picture, where the occupancy of the energetically close-lying σ and π orbitals determines their spin state and philicity.[4] Thus, the spin state, triplet ($S = 1$) or singlet ($S = 0$), depends strongly on the substituents at the carbene center: most alkyl- or aryl-substituted carbenes show a triplet ground state, whereas σ-accepting and π-donating substituents such as O, N, or halogens stabilize the singlet states.

A similar effect is observed for substitution in the para positions of arylcarbenes. Song and Sheridan studied the influence of methoxy substitution on the spin state of triplet phenyl(trifluormethyl)carbene and observed that para substitution leads to a switching of the spin state to singlet, whereas meta substitution does not change the spin state.[5] While fluorenylidene shows a triplet ground state,[6] 3,6-dimethoxyfluorenylidene is a singlet carbene.[7] Diphenylcarbene **1a** exhibits a triplet ground state with a singlet−triplet splitting ΔH_{ST} of 4 kcal/mol in isooctane,[8] whereas for bis(*p*-methoxyphenyl)carbene **1b**, calculations predict that the lowest lying singlet and triplet states should be almost degenerate (Chart 1).

Carbenes **1a** and **1b** are short-lived at room temperature in solution, but they can be isolated at cryogenic temperatures in inert gas matrices or in organic glasses.[9,10] A carbene such as diphenylcarbene **1a** is entirely stable in inert gas matrices, and its bimolecular chemistry can be studied by doping these matrices with small molecules such as O_2,[11,12] CO_2,[13] CO, H_2O,[14] or CH_3OH.[2] Organic glasses are reactive matrices, and at temperatures above 77 K, carbene **1a** decays rapidly, whereas below 50 K, the carbene is stable even in solid alcohols. In 1966, Trozzolo and Gibbons reported that photolysis of the diphenyldiazomethanes **2a** or **2b** in frozen 2-methyltetrahydrofuran (MTHF) at 77 K results in the formation of the corresponding carbenes in their triplet states, T-**1a** and T-**1b**,

Received: November 8, 2015
Published: January 14, 2016

DOI: 10.1021/jacs.5b11696
J. Am. Chem. Soc. 2016, 138, 1622−1629

Chart 1. C−C−C Bond Angles at the Carbene Center and Singlet−Triplet Splittings of 1a and *uu*-1b[a]

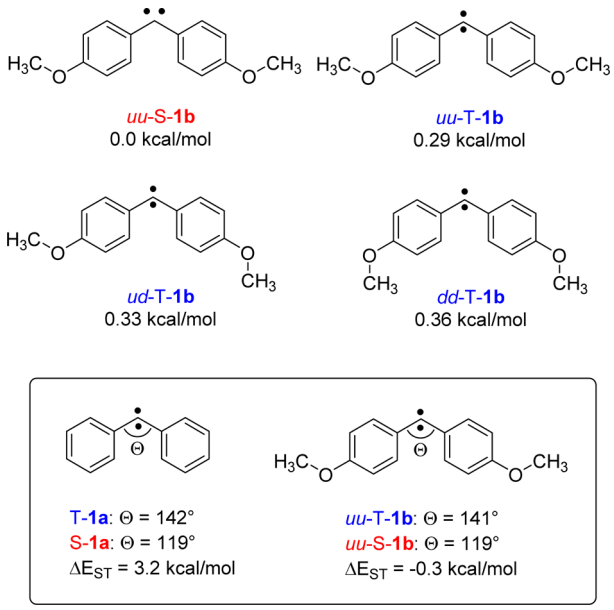

[a]Three conformers of **1b** were considered with respect to the position of the methoxy group: down−down (*dd*), up−down (*ud*), and up−up (*uu*). Energies relative to *uu*-S-**1b** and ΔE_{ST} were computed at the CCSD(T)/cc-pVDZ//B3LYP-D3/def2-TZVP level of theory.

respectively.[15] The carbenes were characterized by EPR, UV−vis, and fluorescence spectra. The authors noted that the photolysis of **2b**, in contrast to that of **2a** and several other derivatives studied, proved to be rather anomalous. At low concentrations of **2b**, carbene T-**1b** could not be observed; instead, an EPR-silent intermediate x with a strong absorption at 390 nm was found. The hypothesis that **1b** has a singlet ground state and intermediate x is indeed S-**1b** was ruled out by the observation that at higher concentrations both the unknown compound x and the triplet carbene T-**1b** are formed. From that, a triplet ground state of **1b** was inferred, and it was concluded that "great caution should be exercised in assigning a given absorption to a methylene even if the ESR spectrum has been obtained in different experiments under rather similar conditions".[15] Later, Humphreys and Arnold studied a series of para-substituted diphenylcarbenes including T-**1b** by temperature-dependent EPR spectroscopy, and from the linear Curie−Weiss plot, they also concluded that T-**1b** has a triplet ground state and that S-**1b** is not populated to any significant extent.[16,17]

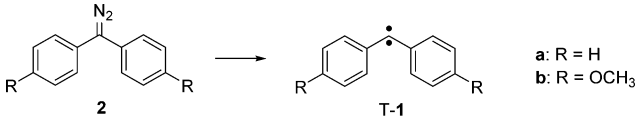

When triplet ground state carbenes are generated by photolysis from singlet precursors such as diazo compounds **2**, the carbenes are initially formed in their singlet (excited) states followed by rapid intersystem crossing (ISC) to the triplet ground state.[1] For diphenylcarbene **1a**, the ISC rate in CH_3CN was determined to be 311 ± 22 ps^{-1} by picosecond fluorescence spectroscopy,[18] which was later confirmed by femtosecond absorption spectroscopy.[19] In nonpolar hydrocarbons as solvents, the ISC rates of **1a** are roughly 3 times faster. Matrix isolation of carbenes produces the carbenes in their thermodynamically most stable electronic ground states, which can be either singlet or triplet. The ISC generally is too fast to allow for the detection of excited spin states under the conditions of matrix isolation. The only exception was reported in 1999 by Bally, McMahon, and co-workers.[20] 2-Naphthyl(carbomethoxy)carbene T-**1c** is a triplet ground state carbene that on irradiation into its weak visible absorption (λ > 515 nm) is transformed into its metastable singlet state, S-**1c**. After several hours in the dark at 12 K or upon 450 nm illumination, S-**1c** is converted back to T-**1c** almost quantitatively. This system is highly complex, since numerous conformers of the carbene and several rearranged products have to be considered. A very careful analysis of the IR, UV−vis, and EPR spectra allowed the authors to conclude that the singlet state S-**1c** is stabilized by obtaining a perpendicular conformation with the carbomethoxy group rotated out of plane and that a barrier between the two states is created by the pronounced conformational change.[20]

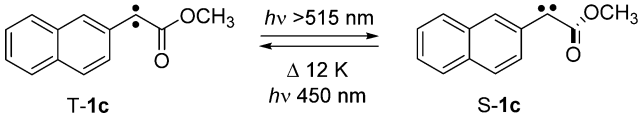

Carbene **1c** was also studied by ultrafast spectroscopy.[21−23] It was found that in cyclohexane as solvent the singlet carbene S-**1c** is converted to T-**1c** with a lifetime of approximately 2 ns. In chloroform, acetonitrile, and Freon-113, on the other hand, singlet S-**1c** is the ground state, and no triplet is formed at all. This indicates that in solid argon, where T-**1c** is the ground state, singlet S-**1c** is stabilized in the rigid matrix cage by restrictions for the large conformational change required during the S−T interconversion.

So far, carbene **1c** has been the only carbene where both the triplet (ground) state and an excited (metastable) singlet state coexist for a period of hours at low temperatures. Recently, we have shown that the singlet state of diphenylcarbene S-**1a** is strongly stabilized by hydrogen bonding and that the hydrogen-bonded S-**1a**···H-OR coexists with T-**1a** in the same matrix.[2,14] In that case, S-**1a**···H-OR is thermodynamically more stable than T-**1a**···H-OR, and T-**1a** is more stable than S-**1a**. However, S-**1a**···H-OR is only metastable, and with a half-lifetime of several hours, it rearranges to the formal O−H insertion product via quantum mechanical tunneling (QMT).

We now report that, in contrast to previous findings,[15−17] carbene **1b** shows a singlet ground state S-**1b** in inert gas matrices as well as in organic glasses. The excited triplet state T-**1b** can be photochemically populated in high yields and is indefinitely stable at very low temperatures. Thus, both the singlet and triplet states of carbene **1b** can be reversibly generated, and the intersystem crossing rate between these states is essentially zero.

RESULTS AND DISCUSSION

EPR and ENDOR Experiments. The diazo compound **2b** was photolyzed using visible light (510 or 530 nm) or UV light (365 nm) in various matrices (Ar, Ne) and organic glasses (MTHF) at cryogenic temperatures (3−10 K), and the products were analyzed by EPR, IR, and UV−vis spectroscopy. The EPR experiments demonstrate that photolysis of **2b** produces T-**1b** with a characteristic triplet spectrum in all matrices, which is dominated by a large zero-field splitting (zfs) due to the anisotropic dipolar interaction of the two electron magnetic moments (see Figure S1A and refs 24 and 25). The

DOI: 10.1021/jacs.5b11696
J. Am. Chem. Soc. 2016, 138, 1622−1629

W-band (94 GHz) EPR spectrum in MTHF at 10 K is shown in Figure 1A. The $m_S = -1 \rightarrow m_S = 0$ transitions (denoted x_{-1}, y_{-1}, z_{-1} in the canonical orientations), extending to the high-field edge of the spectrum, is of larger intensity than the $m_S = 0 \rightarrow m_S = +1$ transitions, extending to the low-field edge (see Figure S1). Thus, the sign of the zfs parameter D is positive, which is characteristic for phenyl-ring-substituted carbenes.[26] Spin-Hamiltonian-based simulations yield zfs parameters of D = 0.4035 cm^{-1} and E = −0.0201 cm^{-1}.

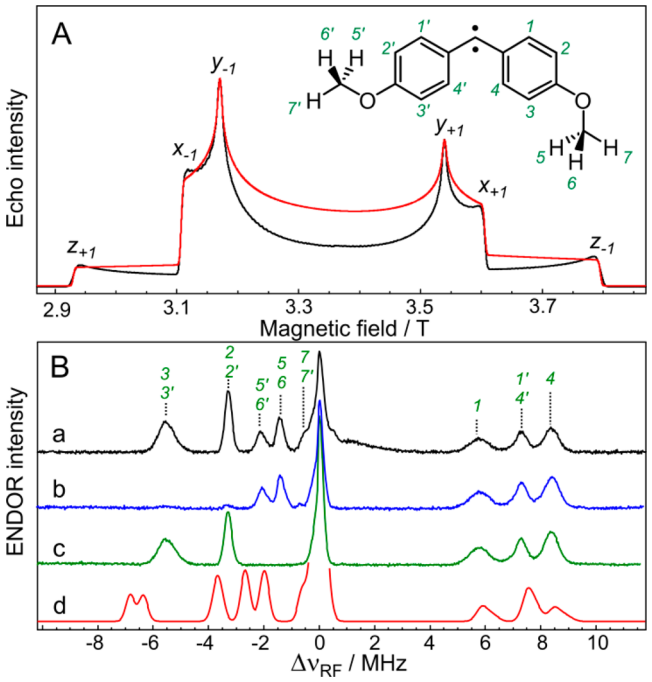

Figure 1. (A) W-band echo-detected EPR spectrum of T-**1b** in MTHF recorded at 10 K (black) and a simulation thereof (red). The canonical magnetic field positions are marked. (B) Q-band ^{1}H Davies ENDOR spectra of (a) T-**1b** in MTHF, (b) T-**1b**-d_4 (deuterated at positions 2, 2′, 3, and 3′), and (c) T-**1b**-d_6 (methyl groups deuterated) in toluene-d_8 measured at 5 K at the z_{+1} EPR spectral position, as well as (d) a simulation for the *ud* conformer of T-**1b**. The numbers above trace a show the assignment of ENDOR lines to corresponding T-**1b** protons as numbered in panel A. The simulation employs the DFT-calculated g and A-tensors and the D tensor, rescaled to match the experimental D, from *ud*-T-**1b**. The spectra in A and B were recorded after 510 nm photolysis of the corresponding (isotopically labeled) diazo precursors **2b** at 10 K. For experimental settings, see Figures S1 (A) and S2 (B).

We employed ENDOR to structurally characterize T-**1b** by means of its ^{1}H /^{2}H electron−nuclear hyperfine interactions, which provides insight into the spin density distribution across the molecule and hence access to its spatial conformations. ENDOR is a very efficient method to observe nuclear spin transitions directly in the radio frequency domain. Two standard ENDOR pulse sequences, Davies and Mims, are usually used for nuclei with large (^{1}H) and small (^{2}H) hyperfine interactions, respectively (see Supporting Information, section 1, and ref 27). The ENDOR spectra for triplet species differ from those of $S = {}^1/_2$ species in that the nuclear resonances are not symmetric around the nuclear Larmor frequency ν_n due to the orientation selectivity resulting from the zfs (see ref 28). Measured at the field positions of the z edges (Figure 1A), the ENDOR spectra are most selective and hence simple. There, the difference $\Delta\nu_{RF}$ between the transition frequency and ν_n corresponds directly to the hyperfine tensor component A_{zz} (z_{-1}) or $-A_{zz}$ (z_{+1}), the magnitude and sign of which can thus be read from the $\Delta\nu_{RF}$ axis.

The Q-band (34 GHz) ^{1}H Davies ENDOR spectrum at z_{+1} of T-**1b** in MTHF at 5 K is shown in Figure 1B, trace a. In addition to the large central line from nuclear transitions within the $m_S = 0$ electronic spin manifold as well as weakly coupled matrix protons, seven well-resolved ENDOR lines are observed. Four of them have transition frequencies lower than the ^{1}H Larmor frequency ($\Delta\nu_{RF} < 0$), whereas the other three have higher frequencies. In analogy to the spin density distribution and ^{1}H hyperfine tensors in T-**1a**,[29,30] the lines at $\Delta\nu_{RF}$ = −5.5 and −3.3 MHz can be assigned to the ring protons 2, 2′, 3, and 3′ having positive hyperfine coupling values (for proton numbering, see Figure 1A). The ENDOR lines at positive $\Delta\nu_{RF}$ stem from the ring protons 1, 1′, 4, and 4′ and correspond to large negative hyperfine couplings.[29,30] The remaining two lines at $\Delta\nu_{RF} \approx -2.2$ and −1.4 MHz must then originate from protons of the methoxy groups. As further proof of the assignment, T-**1b**-d_4 and T-**1b**-d_6, deuterated at positions 2, 2′, 3, and 3′ or at the methoxy groups, respectively, were investigated (Figure 1B, traces c and d). This selective isotopic labeling allows complete assignment of the resonances in both the ^{1}H Davies ENDOR and ^{2}H Mims ENDOR (Figure S2) spectra. The well-resolved ENDOR lines of the protons of the methyl groups clearly reveal that these groups are nonrotating at these temperatures (see also Figure S3).

With respect to the orientations of the methoxy groups, three conformers, *uu*, *ud*, and *dd*, of T-**1b** were considered (Chart 1). According to calculations, these conformers are almost degenerate in energy (Table S10). Their calculated ^{1}H A_{zz} values (Table S1) show that the two different methyl group orientations entail distinct hyperfine couplings in the respective *p*-methoxyphenyl moieties of the molecule. ENDOR simulations employing the parameters from *ud*-T-**1b** (Figure 1B, trace d) reproduce the experimental spectra reasonably well, basically identical to that of a 50:50 mixture of *uu*-T-**1b** and *dd*-T-**1b** (not shown). The peak intensities can be best reproduced by a 40:60 mixture of methoxy group up and down conformations. Thus, considering their similar energies, a mixture of all three conformers, which do not interconvert under the low-temperature experimental conditions, is most likely present in the organic glass.

Photolysis of **2b** in solid argon at 5 K also resulted in the formation of triplet carbene T-**1b**. The X-band (9.5 GHz) EPR spectrum (Figure 2, trace a) was simulated with zfs parameters of D = 0.4096 cm^{-1} and E = −0.0190 cm^{-1} (Figure S4), close to the values measured in MTHF. In the temperature range between 5 and 30 K, a linear signal dependence on the inverse temperature was observed, as expected for a ground-state triplet or nearly degenerate singlet and triplet states (Figure 2, inset). However, if the matrix was cooled back to 5 K after annealing at various higher temperatures for 10 min each, then the original signal intensity could not be recovered, indicating an irreversible reaction of T-**1b** to an EPR-silent singlet species. After annealing for 10 min at 8 K, the loss was 10%, at 15 K 33%, at 20 K 48%, and at 30 K 69% (Figure S5). Irradiation at 5 K with λ = 365 nm resulted in a recovery of T-**1b**, and this behavior was reproducible in repeated annealing/irradiation cycles. This indicates that annealing of the matrix results in the formation of an EPR-silent reservoir compound of T-**1b**, from which the triplet carbene can be restored by UV irradiation. Interestingly, the 365 nm irradiation produces, in addition to

DOI: 10.1021/jacs.5b11696
J. Am. Chem. Soc. 2016, 138, 1622−1629

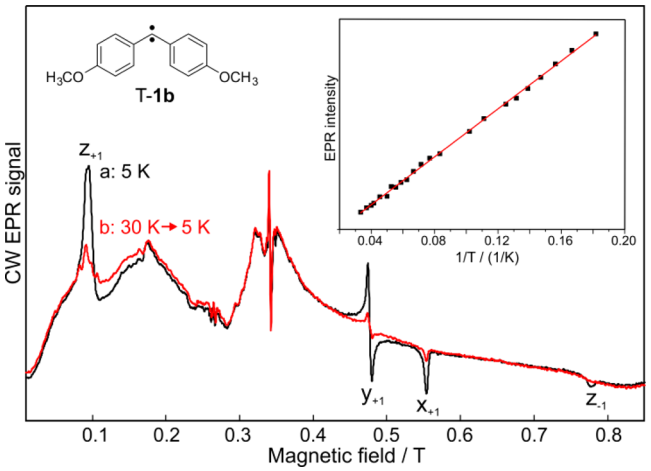

Figure 2. X-band CW EPR spectra of an argon matrix showing the decrease of signal intensity of T-**1b** after warming from 5 to 30 K and cooling back to 5 K. (a) Argon matrix at 5 K showing the triplet spectrum of T-**1b** (black line; zfs parameters D = 0.4096 cm^{-1} and E = −0.0190 cm^{-1}). (b) After annealing at 30 K for 10 min and cooling back to 5 K, 69% of the signal intensity is lost (red line). Inset: EPR signal intensity plotted vs inverse temperature.

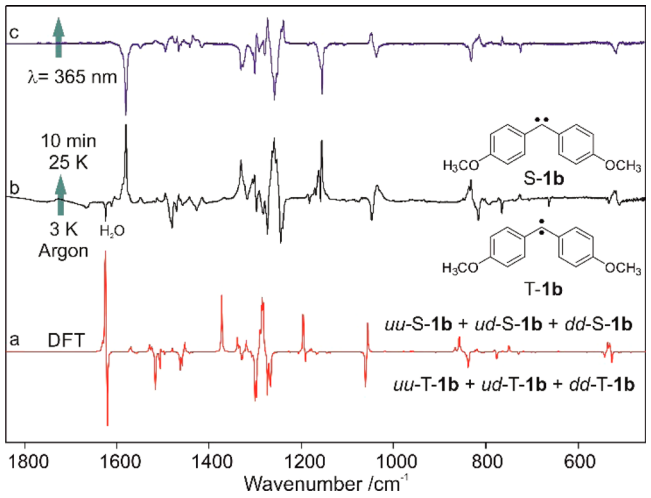

Figure 3. IR spectra showing the thermal interconversion of T-**1b** to S-**1b**. (a) Difference spectrum showing the interconversion of T-**1b** to S-**1b** calculated at the B3LYP-D3/def2-TZVP level of theory (red line). Equal contributions of the three conformers, *dd*, *ud*, and *uu*, were used to simulate the IR spectrum. (b) Difference spectrum at 3 K showing changes after 10 min annealing of an argon matrix containing both T-**1b** and S-**1b** at 25 K (black line). Bands pointing downward, assigned to T-**1b**, are disappearing, and bands pointing upward, assigned to S-**1b**, are appearing. (c) Difference spectrum at 3 K showing changes after 10 min of 365 nm irradiation of the same matrix. Bands pointing downward, assigned to S-**1b**, are disappearing, and bands pointing upward, assigned to T-**1b**, are appearing.

the original EPR signals assigned to T-**1b**, a second triplet with slightly different zfs parameters (D = 0.4053 cm^{-1} and E = −0.0173 cm^{-1}; Figure S6). Most likely, this second triplet is due to a different conformer of T-**1b** formed upon 365 nm irradiation. A similar loss of intensity of the triplet signals was observed during annealing of MTHF glasses. However, since MTHF is a reactive matrix, signal loss could also arise from reactions with the matrix, which is excluded in argon matrices.

IR Spectra. To shed light on the unexpected thermal behavior of T-**1b** in solid argon, the photolysis of matrix-isolated **2b** was investigated by IR spectroscopy. Visible-light irradiation (530 nm) of **2b** matrix-isolated in argon at 3 K resulted in the disappearance of its characteristic C═N═N stretching vibration and formation of a complex spectrum (Figure S8, traces a and b). Comparison of the spectrum with that of the three triplet conformers calculated at the B3LYP-D3/def2-TZVP level of theory (Figure S8, traces c–e) reveals the formation of a mixture of conformers plus additional compounds clearly differing from T-**1b**. Annealing of the matrix at 25 K for several minutes results in a substantial change in the IR spectrum (Figure 3, trace b): all bands assigned to the conformers of T-**1b** decrease in intensity, and those of the additional compounds increase. By comparison with DFT calculations (Figure 3, trace a), we assign these additional compounds to the singlet state of the carbene, S-**1b**. At 3 K, the singlet and triplet states of carbene **1b** coexist in the matrix, and there is no thermal interconversion between these states on a time scale of hours. However, the interconversion can be induced photochemically: 365 nm irradiation results in an increase of T-**1b** (Figure 3, trace c), whereas 450 nm irradiation leads to an increase of S-**1b** (Figure S10, trace d).

A quantitative evaluation of the IR spectra (Table S8) reveals that the 530 nm photolysis of precursor **2b** results in a percent ratio of S-**1b**/T-**1b** of approximately 50:50. This ratio is independent of both the irradiation time (several minutes to hours) and the extent of **2b** converted to **1b** (small fraction or complete). This indicates that either (i) the 530 nm photolysis of **2b** produces the singlet and triplet carbene in a single step with a branching ratio of approximately 50:50 or (ii) S-**1b** and T-**1b** are formed in a photostationary equilibrium, where the photoequilibration is more efficient and faster than the photolysis of **2b**. Annealing at 25 K for 10 min increases the singlet/triplet percent ratio to 75:25. Subsequent UV irradiation (365 nm) for 10 min decreases the ratio to 60:40, and visible-light illumination (450 nm) for 10 min increases it again to 75:25. Prolonged 365 nm irradiation (several hours) leads to S-**1b**/T-**1b** ratios greater than 20:80. Thus, depending on the wavelength of irradiation, matrices containing preferentially either S-**1b** or T-**1b** can be produced, and at 3 K, no thermal interconversion between the singlet and triplet states is observed. These observations are in complete agreement with the EPR experiments described above, and the EPR-silent reservoir compound of T-**1b** is therefore identified as the singlet state S-**1b**. There is some evidence from the EPR and IR spectra that the 450 nm irradiation is conformer-selective (in the EPR, the minor triplet with D = 0.4053 cm^{-1} and E = −0.0173 cm^{-1} is bleached preferentially; Figure S7); however, the data do not allow us to determine which of the conformers is photoconverted preferentially.

UV–Vis Spectra. The same type of experiments as described above were conducted with UV–vis detection (Figure 4). In argon at 8 K, the diazo compound **2b** shows two strong bands at 280 and 230 nm and a very weak band at 535 nm (assigned to the n → π^* transition of **2b**), which decrease upon 530 nm photolysis. Simultaneously, a weak band at 483 nm and two medium strong and broad bands at 384 and 316 nm appear during the photolysis. Annealing at 25 K results in a decrease of the bands at 483 and 316 nm, which are therefore assigned to T-**1b**, and an increase of the 384 nm absorption, assigned to S-**1b** (Figure S12B). Subsequent irradiation with UV light (365 nm) results in a decrease of the S-**1b** absorption at 384 nm and an increase of the T-**1b**

DOI: 10.1021/jacs.5b11696
J. Am. Chem. Soc. 2016, 138, 1622–1629

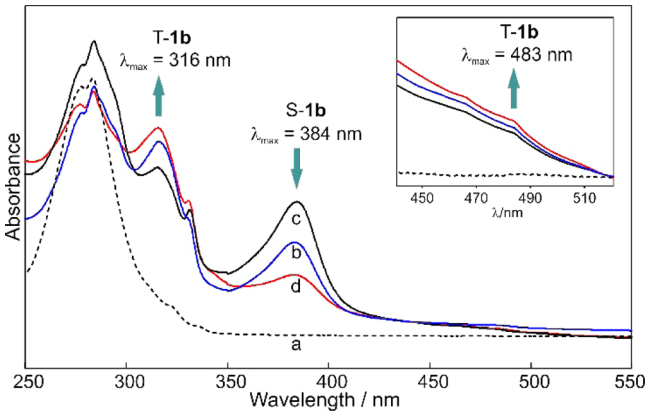

Figure 4. UV−vis spectra showing interconversion of 2**b**, T-**1b**, and S-**1b** by irradiation and annealing. (a) UV−vis spectrum of **2b** isolated in argon matrix at 8 K (dotted line). (b) UV−vis spectrum obtained after several hours of 530 nm irradiation of **2b** at 8 K (blue line). (c) UV−vis spectrum of the same matrix after 10 min annealing to 25 K and cooling back to 8 K (black line). (d) UV−vis spectrum after subsequent 10 min irradiation with λ = 365 nm (red line). The band of S-**1b** decreases, whereas those of T-**1b** increase during irradiation (indicated by green arrows). The weak band of T-**1b** in the visible region of the spectrum is shown in the inset (intensity multiplied by 20).

bands (Figure 4), whereas visible-light (450 nm) irradiation results in an increase of the 384 nm absorption of S-**1b** and a decrease of the bands of T-**1b** (Figure S13). A quantitative analysis of the UV−vis spectra obtained under various conditions (irradiation wavelengths, matrix temperature; Table S9) revealed very similar ratios of S-**1b**/T-**1b** as those found in the corresponding IR experiments (see above).

With only T-**1b** absorbing in the visible range of the spectrum (483 nm), visible-light irradiation drives the photostationary equilibrium toward S-**1b**. On the other hand, irradiation into the strong 384 nm band of S-**1b** shifts the equilibrium toward T-**1b**. Thus, the absorption characteristics of the two states of **1b** allow the observed photochemical behavior to be straightforwardly rationalized.

DFT Calculations. The singlet−triplet gap ΔE_{ST} of carbene **1b** depends mainly on the C−C−C bond angle at the carbene center. However, the question remains as to how the conformational flexibility of the methoxy groups influences ΔE_{ST}. Therefore, the S-**1b** and T-**1b** conformers *dd*, *ud*, and *uu* were computed at the CCDS(T)/cc-pVDZ//B3LYP-D3/def2-TZVP level of theory. The results reveal that the orientation of the methoxy groups has basically no influence on the relative stability of the conformers in the singlet or triplet state (Table S10). With respect to ΔE_{ST}, S-**1b** is estimated to be 0.24−0.36 kcal/mol more stable than T-**1b**, considering all combinations of conformers (Table S11). This is in qualitative agreement with the experiments indicating that the singlet state is slightly more stable than the triplet.

The influence of the rotations of the methoxy (C_{phenyl}−O) and methyl (C_{methyl}−O) groups on ΔE_{ST} was also investigated (Figures S16 and S17). Potential energy scans show that the rotations of the methoxy and methyl groups have small influence on the singlet−triplet gap (variations of 1 and 0.1 kcal/mol, respectively). Furthermore, at no point in these scans do singlet and triplet surfaces cross each other, indicating that changes of these internal coordinates are not related to ISC in this system.

Calculations of the energies of *uu*-S-**1b** and *uu*-T-**1b** as a function of the C−C−C bond angle at the carbene center (relaxed scan) reveal a minimum for the singlet at 119° with the triplet lying about 9 kcal/mol higher at the same bond angle (Figure 5). The minimum of the triplet is found at a C−C−C

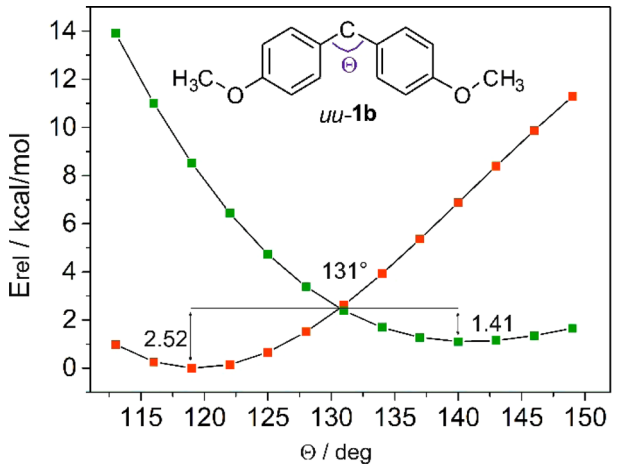

Figure 5. Energy profiles of the scans performed on the C−C−C carbene angles of the *uu* conformers in the triplet (green) and singlet (red) states. The scans were performed at the B3LYP-D3/def2-TZVP level of theory, and the energies were corrected using single-point CCSD(T)/cc-pVDZ calculations.

bond angle of approx 140°, at which angle the singlet is higher in energy. Thus, at the geometry of the singlet, the singlet is more stable than the triplet, and vice versa. The crossing was located at a C−C−C bond angle of 131°, 2.52 kcal/mol above *uu*-S-**1b** and 1.41 kcal/mol above *uu*-T-**1b**. These calculations indicate that an activation barrier of approx 1.4 kcal/mol has to be overcome to convert *uu*-T-**1b** into the more stable *uu*-S-**1b**.

Reaction of 1b with Water. In previous publications, we have shown that the singlet state of diphenylcarbene S-**1a** is strongly stabilized by hydrogen bonding, whereas the triplet state T-**1a** is only weakly interacting.[2,14] In the case of **1b**, both the singlet and triplet carbenes are present in the matrix after photolysis of **2b**. Annealing at temperatures above 20 K is required to allow for the diffusion of matrix-isolated water. At these temperatures, we also observe the ISC of T-**1b** to S-**1b** in the absence of water and therefore water will interact with both T-**1b** and S-**1b**. We expect that S-**1b** strongly interacts with water under formation of the hydrogen-bonded complex S-**1b**···HOH, whereas T-**1b** only weakly interacts, but this weakly bound complex rapidly interconverts to the S-**1b**···HOH complex (Scheme 1).

To assess the influence of water on the singlet−triplet gap, several water complexes were computed while considering not only the carbene center as a potential H-bond acceptor but also both of the oxygen atoms of the methoxy groups. Thus, in addition to 1:1, we also considered 3:1 complexes involving all of the possible acceptor centers at once (Figures S18 and S19). When the oxygen atoms act as acceptors, the effect on the S−T gap is relatively small (~1 kcal/mol), with the triplet complexes being more stabilized than the complexes with the singlet. When the interaction takes place through the carbene center, this situation changes. The singlet carbene is a stronger base than the triplet, with the stabilization energy for the singlet complexes being about 6 kcal/mol larger. This difference in stabilization energies ensures that the singlet remains the

DOI: 10.1021/jacs.5b11696
J. Am. Chem. Soc. 2016, 138, 1622−1629

Scheme 1. S−T Interconversion and Reaction of Carbene 1b with Water

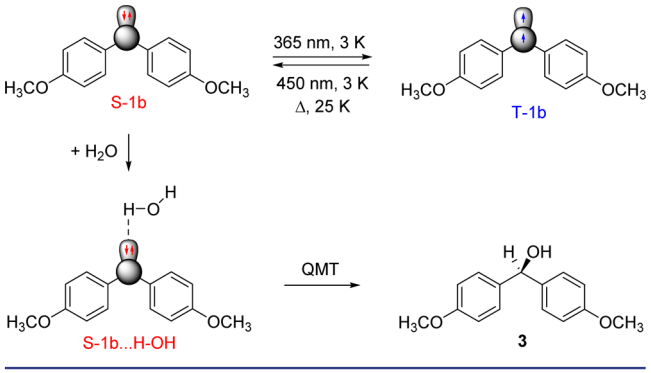

ground state upon interaction with a single water molecule, actually increasing the gap to −5.9 kcal/mol (Table S12). When the interaction with multiple water molecules is considered (3:1 complexes), the stabilization energy of the singlet complexes is again higher than that for the triplet complexes. This results again in a widening of the singlet−triplet gap. The predicted value of the gap in the quaternary complex (−5.2 kcal/mol) is slightly smaller than that for the 1:1 complexes (Table S13). This small difference can be rationalized by the effect of the hydrogen bonding with the methoxy groups, which somewhat tends to stabilize triplet states over singlets. Still, it is not enough to overcome the larger effect of the interaction of water at the carbene center that strongly stabilizes the singlet.

If a 1% H_2O-doped argon matrix containing carbene **1b** (S, T mixture as described above) is warmed from 3 to 25 K, then all bands of T-**1b** decrease in intensity and S-**1b**···HOH is formed (Figure 6). As expected, the IR spectrum of S-**1b** in the complex is only slightly disturbed upon complexation with water. The largest shift of +7.7 cm^{-1} is found for the strong band of S-**1b** at 1339 cm^{-1} (Figure S11), assigned to the unsymmetrical C−C−C stretching vibration involving the carbene center. Since the water molecule is attached to the carbene center, this vibration is affected most. The other vibrations are shifted between 0 and 6 cm^{-1}. Whether S-**1b**··· HOH is formed by the direct interaction of water with S-**1b** or via ISC of the weakly bound T-**1b**···HOH, or by both mechanisms, cannot be determined from our experiments.

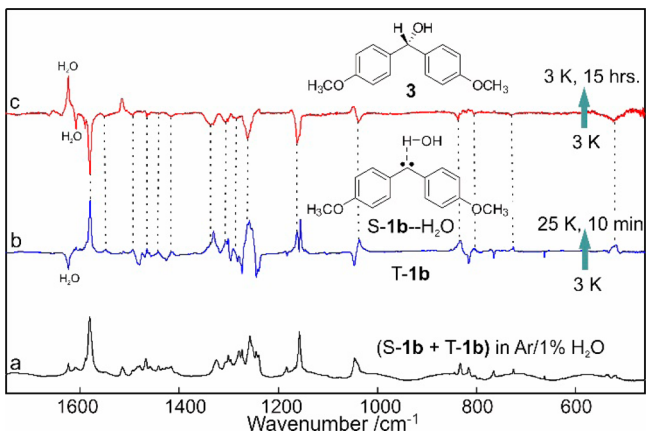

Figure 6. IR spectra showing the formation and degradation of the complex between S-**1b** and water. (a) Mixture of T-**1b** and S-**1b** in an argon matrix doped with 1% H_2O at 3 K (black line). (b) Difference IR spectrum of the same matrix showing changes after annealing for 10 min at 25 K (blue line). Bands pointing downward, assigned to T-**1b**, are disappearing, and bands pointing upward, assigned to the complex S-**1b**···HOH, are appearing. (c) Difference IR spectrum of the same matrix showing changes after 15 h at 3 K (red line). Bands pointing downward are assigned to S-**1b**···HOH, and bands pointing upward are assigned to the O−H insertion product **3**.

The most striking difference between S-**1b** and S-**1b**···HOH is that the singlet carbene S-**1b** is thermally stable as long as it is matrix-isolated, whereas its water complex is only metastable even at 3 K and slowly rearranges with a rate of $7 \pm 3 \times 10^{-6}$ s^{-1} to alcohol **3** (Scheme 1 and Table S5), the formal OH insertion product. The corresponding reaction pathways were computed for the complexes of the three S-**1b** conformers with water (Table S14 and Figure S20). The predicted transition states were very similar to those previously reported for S-**1a**··· HOH, involving a proton transfer from the water molecule to the carbene center followed by barrierless recombination to yield the corresponding alcohol. This is in complete agreement with the behavior of S-**1a**···HOH, which, at similar rates, rearranges to the corresponding alcohol (benzhydrol) via quantum mechanical tunneling.[14] Given the calculated activation barrier for the insertion of S-**1b** into water of 6.3 kcal/mol, we assume that this reaction at 3 K also proceeds via tunneling. The strikingly different kinetic behavior of S-**1b** and its water complex S-**1b**···HOH easily allows these species to be discriminated and the spectra to be assigned even in spectral regions with overlapping absorptions.

CONCLUSIONS

The thermal and photochemical interconversion between the singlet and triplet states of carbene **1b** has been investigated by EPR, IR, and UV−vis spectroscopy in solid argon, by EPR and ENDOR spectroscopy in MTHF, and by theoretical methods. These experiments clearly demonstrate that (i) the singlet and triplet states of carbene **1b** coexist in argon at 3 K and that there is no ISC within the time scale of our experiments (hours). (ii) At 3 K in argon, photostationary equilibria between S-**1b** and T-**1b** are established by irradiation either into the strong UV absorption of S-**1b** or into the weak visible absorption of T-**1b**. Thus, visible-light irradiation (450 nm) shifts the equilibrium toward S-**1b**, and UV irradiation (365 nm), toward T-**1b**. (iii) Annealing at slightly higher temperatures (10−25 K in argon) results in a conversion to S-**1b**, from which we conclude that S-**1b** is thermodynamically more stable than T-**1b** and that these states are separated by an activation barrier that prevents interconversion at 3 K.

In MTHF, the triplet disappears completely above 50 K and can be restored by UV irradiation at 5 K. However, since MTHF is reactive toward carbenes and T-**1b** might be formed by photolysis from remaining precursor **2b**, these experiments are less conclusive than the experiments in argon. Trozzolo and Gibbons investigated the photochemistry of **2b** in MTHF at 77 K in 1966[15] and found, besides T-**1b**, an unknown singlet compound with a strong absorption maximum at 390 nm, which is close to the band at 384 nm that we assign to S-**1b**. Although these authors explicitly ruled out the presence of S-**1b** in their experiments, it is now clear that both S-**1b** and T-**1b** were formed in these early experiments.

Obvious questions are: Why is the ISC in carbene **1b** extremely slow and why can both states coexist in solid argon? Singlet−triplet bistability has been predicted[31,32] and observed previously for diradicals such as N-substituted 3,4-dimethyl-

DOI: 10.1021/jacs.5b11696
J. Am. Chem. Soc. 2016, 138, 1622−1629

enepyrrole biradicals[33] or bis(aminoxyl)diradicals.[34] The only carbene that shows similar behavior is **1c**.[20] However, this carbene has a triplet ground state and the singlet state is kinetically unstable and slowly decays back to the triplet state in the dark. In **1c**, the singlet exhibits a very different geometry with the carbomethoxy group rotated out of plane; thus, the S−T interconversion requires a major geometrical change, which slows the ISC in rigid matrices. In contrast, in **1b** the main geometric difference is the C−C−C bond angle at the carbene center, which increases from 119° in S-**1b** to approx 140° in T-**1b**. This is typical for all carbenes, where the (closed-shell) singlets show narrower bond angles (typically 100−110°) and the triplets wider angles (120−150°); therefore, in this respect, carbene **1b** does not differ from any other carbene. The only difference is that in **1b** the singlet and triplet states are essentially degenerate. At both the geometry of S-**1b** and T-**1b**, the vertical excitation energies to the excited triplet and singlet states, respectively, are large, and the DFT calculations suggest that a thermal barrier of 1.4 kcal/mol has to be overcome for the ISC to occur. While the calculated values might be a rough estimation only, the qualitative predictions are in excellent agreement with the experimental observations: S-**1b** is predicted to be slightly more stable than T-**1b**, and a small thermal activation barrier prevents the interconversion at extremely low temperatures.

In summary, it could be demonstrated that for carbene **1b** the lowest-energy singlet and triplet states coexist. We predict that this bistability of states of different spin multiplicity results from the near degeneracy of these states and therefore should be a general phenomenon in similar systems. In a bistable carbene, the magnetic properties of the system can be switched by irradiation with light of different color and thus this property might be of general interest for applications such as information storage.

EXPERIMENTAL SECTION

Pulse EPR Spectroscopy. W-band (≈94 GHz) pulse EPR measurements were carried out at 10 K using a Bruker ELEXSYS E680 spectrometer employing a home-built ENDOR microwave cavity, which comprised a solenoid of Teflon-coated silver wire integrated into a commercial W-band ENDOR probe head (Bruker). Q-band (≈ 34 GHz) pulse EPR and ENDOR experiments were performed at 5 K using a Bruker ELEXSYS E580 spectrometer equipped with a home-built TE_{011} microwave cavity,[35] a cryogen-free closed-cycle cryostat (Cryogenic Limited) with a Cryomech liquid He compressor, and an ENI 3200L radio frequency (RF) amplifier. For further details about pulse sequences, spectral simulations, and DFT calculations of EPR parameters, see the Supporting Information.

Matrix Isolation Technique. Matrix isolation experiments were performed by standard techniques. For cooling the spectroscopic windows to cryogenic temperatures (3 K or higher), a Sumitomo Heavy Industries two-staged closed-cycle helium cryostat (cooling power 1 W at 4 K) was used. The cryostat was evacuated using a diffusion oil pump for IR experiments, whereas a turbomolecular pump was used for X-band CW EPR experiments. Matrices were generated by co-deposition of **2b** with a large excess of argon (Messer Griesheim, 99.99%) with a flow rate of approximately 1.80 sccm on the top of spectroscopic windows cooled to the lowest temperatures possible (3 K for IR, 8 K for UV−vis, and 5 K for EPR). **2b** was sublimed at 80 °C and co-deposited on the spectroscopic window with a large excess of argon. The temperature of the windows was controlled by an Oxford ITC4 temperature controller. The experiments in 1% water-doped argon matrices were carried out as described earlier.[14] Ultrapure water used in these experiments was degassed by several freeze−pump−thaw cycles (for details, see the Supporting Information).

Computational Details. All gas-phase calculations were performed using the B3LYP density functional[36−38] with D3 dispersion corrections. The def2-TZVP basis set[39] was used in the calculations. All gas-phase computations were carried out with the Gaussian 09 program.[40] CCSD(T) single-point calculations were performed using the cc-pVDZ basis set.[41] The MOLPRO program[42] was used for these calculations.

Since it is a well-known fact that B3LYP overestimates the S−T gap of carbenes[43] and that carbene **1b** is expected to have a near-zero S−T splitting, a CCSD(T) correction was added to the computed values. Energy evaluations at the CCSD(T)/cc-pVDZ//B3LYP-D3/def2-TZVP level were performed for the carbenes and the 1:1 carbene/water complexes. The average difference between the DFT and CCSD(T) energies (separately evaluated for singlet and triplet states) was then used to scale the DFT energies (eq 1)

$$E_c = E_{DFT} + \delta \quad (1)$$

where E_c is the corrected energy, E_{DFT} is the zero-point energy (ZPE)-corrected energy computed at the DFT level, and δ is the CCSD(T) correction.

The relaxed scans were carried out by fixing the torsion coordinates in 10° or 15° intervals while reoptimizing the rest of the internal coordinates in each step. For further details, see the Supporting Information.

For materials, synthesis of the diazoprecursors, and preparation of samples for frozen-solution EPR, see the Supporting Information.

ASSOCIATED CONTENT

Supporting Information

The Supporting Information is available free of charge on the ACS Publications website at DOI: 10.1021/jacs.5b11696.

Extended experimental and computational details; additional figures and tables, and Cartesian coordinates (PDF)

AUTHOR INFORMATION

Corresponding Authors

*anton.savitsky@cec.mpg.de (A.S.)
*esanchez@kofo.mpg.de (E.S.-G.)
*wolfram.sander@rub.de (W.S.)

Notes

The authors declare no competing financial interest.

ACKNOWLEDGMENTS

This work was supported by the Cluster of Excellence RESOLV (EXC 1069) funded by the Deutsche Forschungsgemeinschaft (DFG). E.S.-G. also acknowledges a Liebig Stipend of the Fonds der Chemischen Industrie and funding by the SFB 1093 of the DFG.

REFERENCES

(1) Eisenthal, K. B.; Moss, R. A.; Turro, N. J. *Science* **1984**, *225*, 1439.
(2) Costa, P.; Sander, W. *Angew. Chem., Int. Ed.* **2014**, *53*, 5122.
(3) Etter, R. M.; Skovronek, H. S.; Skell, P. S. *J. Am. Chem. Soc.* **1959**, *81*, 1008.
(4) Chen, B.; Rogachev, A. Y.; Hrovat, D. A.; Hoffmann, R.; Borden, W. T. *J. Am. Chem. Soc.* **2013**, *135*, 13954.
(5) Song, M.-G.; Sheridan, R. S. *J. Am. Chem. Soc.* **2011**, *133*, 19688.
(6) Brandon, R. W.; Closs, G. L.; Davoust, C. E.; Hutchison, C. A., Jr.; Kohler, B. E.; Silbey, R. *J. Chem. Phys.* **1965**, *43*, 2006.
(7) Chuang, C.; Lapin, S. C.; Schrock, A. K.; Schuster, G. B. *J. Am. Chem. Soc.* **1985**, *107*, 4238.
(8) Eisenthal, K. B.; Turro, N. J.; Sitzmann, E. V.; Gould, I. R.; Hefferon, G.; Langan, J.; Cha, Y. *Tetrahedron* **1985**, *41*, 1543.
(9) Sander, W.; Bucher, G.; Wierlacher, S. *Chem. Rev.* **1993**, *93*, 1583.

DOI: 10.1021/jacs.5b11696
J. Am. Chem. Soc. 2016, 138, 1622−1629

(10) Sander, W. W.; Patyk, A.; Bucher, G. *J. Mol. Struct.* **1990**, *222*, 21.
(11) Sander, W. *Angew. Chem., Int. Ed. Engl.* **1986**, *25*, 255.
(12) Sander, W. W. *J. Org. Chem.* **1989**, *54*, 333.
(13) Wierlacher, S.; Sander, W.; Liu, M. T. H. *J. Org. Chem.* **1992**, *57*, 1051.
(14) Costa, P.; Fernandez-Oliva, M.; Sanchez-Garcia, E.; Sander, W. *J. Am. Chem. Soc.* **2014**, *136*, 15625.
(15) Trozzolo, A. M.; Gibbons, W. A. *J. Am. Chem. Soc.* **1967**, *89*, 239.
(16) Humphreys, R. W. R.; Arnold, D. R. *Can. J. Chem.* **1977**, *55*, 2286.
(17) Humphreys, R. W. R.; Arnold, D. R. *Can. J. Chem.* **1979**, *57*, 2652.
(18) Eisenthal, K. B.; Turro, N. J.; Aikawa, M.; Butcher, J. A., Jr.; DuPuy, C.; Hefferon, G.; Hetherington, W.; Korenowski, G. M.; McAuliffe, M. J. *J. Am. Chem. Soc.* **1980**, *102*, 6563.
(19) Peon, J.; Polshakov, D.; Kohler, B. *J. Am. Chem. Soc.* **2002**, *124*, 6428.
(20) Zhu, Z. D.; Bally, T.; Stracener, L. L.; McMahon, R. J. *J. Am. Chem. Soc.* **1999**, *121*, 2863.
(21) Wang, J. L.; Likhotvorik, I.; Platz, M. S. *J. Am. Chem. Soc.* **1999**, *121*, 2883.
(22) Wang, Y. H.; Yuzawa, T.; Hamaguchi, H. O.; Toscano, J. P. *J. Am. Chem. Soc.* **1999**, *121*, 2875.
(23) Zhang, Y.; Kubicki, J.; Wang, J.; Platz, M. S. *J. Phys. Chem. A* **2008**, *112*, 11093.
(24) Carrington, A.; McLachlan, A. D. *Introduction to Magnetic Resonance*; Harper & Row: New York, 1967.
(25) Gerson, F.; Huber, W. *Electron Spin Resonance Spectroscopy of Organic Radicals*; Wiley-VCH: Weinheim, Germany, 2003.
(26) Sinnecker, S.; Neese, F. *J. Phys. Chem. A* **2006**, *110*, 12267.
(27) Schweiger, A.; Jeschke, G. *Principles of Pulse Electron Paramagnetic Resonance*; Oxford University Press: Oxford, 2001.
(28) Kurreck, H.; Kirste, B.; Lubitz, W. *Electron Nuclear Double Resonance Spectroscopy of Radicals in Solution: Application to Organic and Biological Chemistry*; Wiley: New York, 1988.
(29) Anderson, R. J. M.; Kohler, B. E. *J. Chem. Phys.* **1976**, *65*, 2451.
(30) Hutchison, C. A.; Kohler, B. E. *J. Chem. Phys.* **1969**, *51*, 3327.
(31) Shaik, S. S.; Hiberty, P. C. *A Chemist's Guide to Valence Bond Theory*; Wiley: Hoboken, NJ, 2007.
(32) Dias, J. R. *Mol. Phys.* **2013**, *111*, 735.
(33) Bush, L. C.; Heath, R. B.; Feng, X. W.; Wang, P. A.; Maksimovic, L.; Song, A. I.; Chung, W. S.; Berinstain, A. B.; Scaiano, J. C.; Berson, J. A. *J. Am. Chem. Soc.* **1997**, *119*, 1406.
(34) Rajca, A.; Lu, K.; Rajca, S.; Ross, C. R., II *Chem. Commun. (Cambridge, U. K.)* **1999**, 1249.
(35) Reijerse, E.; Lendzian, F.; Isaacson, R.; Lubitz, W. *J. Magn. Reson.* **2012**, *214*, 237.
(36) Becke, A. *J. Chem. Phys.* **1993**, *98*, 5648.
(37) Lee, C.; Yang, W.; Parr, R. G. *Phys. Rev. B: Condens. Matter Mater. Phys.* **1988**, *37*, 785.
(38) Grimme, S.; Antony, J.; Ehrlich, S.; Krieg, H. *J. Chem. Phys.* **2010**, *132*, 154104.
(39) Weigend, F.; Haser, M.; Patzelt, H.; Ahlrichs, R. *Chem. Phys. Lett.* **1998**, *294*, 143.
(40) Frisch, M. J.; Trucks, G. W.; Schlegel, H. B.; Scuseria, G. E.; Robb, M. A.; Cheeseman, J. R.; Scalmani, G.; Barone, V.; Mennucci, B.; Petersson, G. A.; Nakatsuji, H.; Caricato, M.; Li, X.; Hratchian, H. P.; Izmaylov, A. F.; Bloino, J.; Zheng, G.; Sonnenberg, J. L.; Hada, M.; Ehara, M.; Toyota, K.; Fukuda, R.; Hasegawa, J.; Ishida, M.; Nakajima, T.; Honda, Y.; Kitao, O.; Nakai, H.; Vreven, T.; Montgomery, J. A., Jr.; Peralta, J. E.; Ogliaro, F.; Bearpark, M.; Heyd, J. J.; Brothers, E.; Kudin, K. N.; Staroverov, V. N.; Kobayashi, R.; Normand, J.; Raghavachari, K.; Rendell, A.; Burant, J. C.; Iyengar, S. S.; Tomasi, J.; Cossi, M.; Rega, N.; Millam, J. M.; Klene, M.; Knox, J. E.; Cross, J. B.; Bakken, V.; Adamo, C.; Jaramillo, J.; Gomperts, R.; Stratmann, R. E.; Yazyev, O.; Austin, A. J.; Cammi, R.; Pomelli, C.; Ochterski, J. W.; Martin, R. L.; Morokuma, K.; Zakrzewski, V. G.; Voth, G. A.; Salvador, P.; Dannenberg, J. J.; Dapprich, S.; Daniels, A. D.; Farkas, O.; Foresman, J. B.; Ortiz, J. V.; Cioslowski, J.; Fox, D. J. *Gaussian 09*, revision B.01; Gaussian, Inc.: Wallingford, CT, 2009.
(41) Dunning, T. H. *J. Chem. Phys.* **1989**, *90*, 1007.
(42) Werner, H.-J.; Knowles, P. J.; Knizia, G.; Manby, F. R.; Schütz, M. *Wiley Interdisciplinary Reviews: Computational Molecular Science* **2012**, *2*, 242.
(43) Woodcock, H. L.; Moran, D.; Brooks, B. R.; Schleyer, P. v. R.; Schaefer, H. F., III *J. Am. Chem. Soc.* **2007**, *129*, 3763.

DOI: 10.1021/jacs.5b11696
J. Am. Chem. Soc. 2016, 138, 1622−1629